Journal of Alloys and Compounds 509 (2011) 1953–1957

Contents lists available at ScienceDirect

Journal of Alloys and Compounds

journal homepage: www.elsevier.com/locate/jallcom

Photocatalytic and microwave absorbing properties of polypyrrole/Fe-doped TiO_2 composite by in situ polymerization method

Qiaoling Li*, Cunrui Zhang, Jianqiang Li

Department of Chemistry, North University of China, Taiyuan 030051, China

ARTICLE INFO

Article history:
Received 13 March 2010
Received in revised form 21 October 2010
Accepted 21 October 2010
Available online 30 October 2010

Keywords:
Fe-doped TiO_2
Polypyrrole
Microwave absorbing
Photocatalysis

ABSTRACT

The Fe-doped TiO_2 microbelts were prepared by sol–gel method using the absorbent cotton template for the first time. Then the Fe-doped TiO_2 microbelts were used as templates for the preparation of polypyrrole/Fe-doped TiO_2 composites. Polypyrrole/Fe-doped TiO_2 composites were prepared by in situ polymerization of pyrrole on the Fe-doped TiO_2 template. The structure, morphology and properties of the composites were characterized with scanning electron microscope (SEM), FTIR, Net-work Analyzer. The possible formation mechanisms of Fe-doped TiO_2 microbelts and polypyrrole/Fe-doped TiO_2 composites have been proposed. The effect of the molar ratio of pyrrole/Fe-doped TiO_2 on the photocatalytic properties and microwave loss properties of the composites was investigated.

1. Introduction

New technologies demand materials and structures with specially tailored properties. Heterostructures consisting of composites of titanium dioxide (TiO_2) and organic conducting polymers have gained a considerable interest in research and development of many practicable applications, such as lithium ion batteries (TiO_2-PPY [1]), photocatalytic activity (TiO_2-PPY [2,3]), electrorheological fluids (TiO_2-PANI [4]), biosensors (TiO_2-PANI [5]), rectification diodes (TiO_2-PANI [6]) and solid-state solar cells (TiO_2-PANI [7,8]). Conducting polymers, like polypyrrole (PPY) and polyaniline (PANI), are of much interest because of their diverse structures, special doping mechanism, excellent environmental stability, good solution processability and high conductivity [9,10]. Among various conducting polymers, polypyrrole is one of the most promising conducting polymers. TiO_2 is widely accepted as one of the most promising photocatalysts and semiconductor because of its high photoactivity, low cost, nontoxicity, and chemical stability [11]. The doping [12–14] and morphologies [15,16] for TiO_2 could improve the photocatalytic efficiency. And conducting polymers such as polypyrrole, polyaniline, and their derivatives are all used as hole conductors to improve the photocatalysis. Doped TiO_2 particle especially the doped TiO_2 microbelt is a photocatalytic material with advantages of low-density, high specific surface area, superior delivering capacity, low price, and facility to mold. Meanwhile doped TiO_2 is an excellent wave-transmitting material, which can widen the frequency bandwidth of microwave absorber. The microwave absorbing properties of the composite can be controlled by use of synthetic metals in the microwave absorber. Besides, the use of embedding microparticles in electroless deposited metals is a convenient method of preparing composite coatings. Some work has been carried out to investigate the effect of operating conditions on the properties of TiO_2 composite coatings [17,18]. However, reports on both photocatalysis properties and the microwave absorbing properties of micro-composite coatings are scanty.

In the present work, the absorbent cotton template was used for preparing Fe-doped TiO_2 microbelts by sol–gel method. Then the doped TiO_2 microbelts were used as templates to prepare the polypyrrole/doped TiO_2 composite in the emulsion polymerization system. The morphology, structure and properties for the Fe-doped TiO_2 microbelts, polypyrrole/Fe-doped TiO_2 composite were also studied in this work.

2. Experimental

2.1. Synthesis of Fe-doped TiO_2 microbelts

Fe-Doped TiO_2 microbelts were prepared by sol–gel method. The detailed process could be described as follows. Tetrabutyl titanate ($Ti(OBu)_4$, 8 mL) were dissolved in 100 mL anhydrous ethanol. The entire mixture was stirred at 30 °C for 0.5 h. Then 1.2 mL acetylacetone was dripped to the above mixture. $Fe(NO_3)_3{\cdot}9H_2O$ (Fe^{3+} doped mass percentage was 0.04%), 15 mL anhydrous ethanol and 0.45 mL HNO_3 were dripped into the mixture. The entire mixture was stirred at 30 °C for 0.5 h. Then the mixture was dropped on the dried absorbent cotton, followed by drying at 30 °C for 5 h. Then the above dried absorbent cotton was heated in an oven in air atmosphere at 600 °C for 2 h to obtain Fe-doped TiO_2 microbelts A.

* Corresponding author. Tel.: +86 351 3923197; fax: +86 351 3922152.
E-mail address: qiaolingl@126.com (Q. Li).

0925-8388/$ – see front matter © 2010 Elsevier B.V. All rights reserved.
doi:10.1016/j.jallcom.2010.10.099

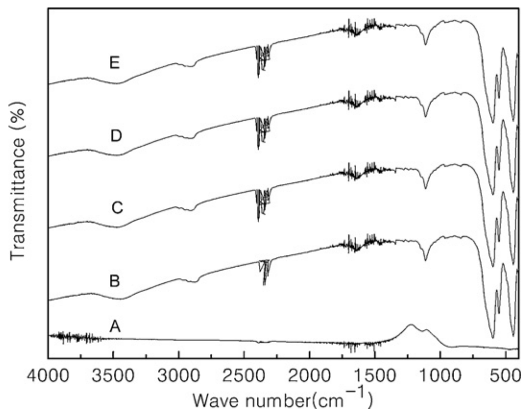

Fig. 1. FTIR spectra of polypyrrole/Fe-doped TiO_2 composite obtained by different molar ratios of pyrrole/Fe-doped TiO_2: (A) 0; (B) 2; (C) 4; (D) 6; (E) ∞.

2.2. Synthesis of polypyrrole/Fe-doped TiO_2 composite

Polypyrrole/Fe-doped TiO_2 composites were prepared in the phase of sodium lauryl benzene sulfate (DBS) emulsion polymerization system. The detailed process could be described as follows. Some amount of Fe-doped TiO_2 was dispersed in sodium lauryl benzene sulfate solution. The pyrrole was added into the above solution, the molar ratios of pyrrole/Fe-TiO_2 were kept at 2:1, 4:1, 6:1, ∞ to obtain sample B, C, D and E, respectively. Then the solution was agitated by magnetic stirring apparatus (RPM = 100) under the atmosphere of nitrogen for 1 h. Then HCl (1.5 mol L^{-1}) and anhydrous $FeCl_3$ (the molar ratio of pyrrole/HCl/$FeCl_3$ was 1:1:2) were added to the pyrrole mixture. Then the mixture was agitated for 24 h at 0–5 °C. The precipitates were washed with ethyl alcohol, HCl (6 mol L^{-1}) and water for many times, respectively. Finally, the product was dried under vacuum at 60 °C for 10 h. Thus the PPY/Fe-doped TiO_2 composites B, C, D and E were obtained.

2.3. Characterization

Fourier transform infrared spectroscopy (FTIR) spectra of the samples were taken in dried KBr powder on Nexus 670 spectrometer (Nicolet, USA). The morphology of the samples was investigated by scanning electron microscope (SEM). The samples for measuring microwave properties were prepared by dispersing the doped TiO_2 micro-belts and polypyrrole/doped TiO_2 composites in paraffin wax, respectively. The volume fraction of the powders is 60%. The powder/wax composites were die-pressed to form cylindrical toroidal specimens with 7.0 mm outer diameter, 3.0 mm inner diameter, and 3 mm thickness. The measurements of microwave loss property for the specimens were carried out using a PNA 3629D vector network analyzer in the 30–6000 MHz ranges.

3. Results and discussion

3.1. FTIR spectral analysis

Molecular structures of the resulting samples were characterized by FTIR spectra in the range from 4000 to 400 cm^{-1}. The FTIR spectra of the Fe-doped TiO_2 and polypyrrole/Fe-doped TiO_2 composites are shown in Fig. 1. For polypyrrole/Fe-doped TiO_2 composites, it could be found that the characteristic peaks corresponding to the TiO_2 (the wide peaks at the range from 400 cm^{-1} to 800 cm^{-1}). And there are no the characteristic peaks corresponding to the Fe-doped TiO_2 appeared in the curve B, C, D, E of the Fig. 1, indicating the Fe-doped TiO_2 microbelt was enwrapped by the PPY completely. Additionally, the band at 3450 cm^{-1} is attributable to N–H stretching mode. The peaks at 1560 cm^{-1} and 1470 cm^{-1} corresponding to the characteristic C=C stretching of the pyrrole rings [19,20] are also observed in curves B, C, D, E of Fig. 1. The peak around 1134 cm^{-1} is associated with vibrational modes of N=Q=N (Q refers to the pyrrole-type rings), indicating that PPY formed in the composites sample.

3.2. Morphology and formation mechanism of the samples

3.2.1. Formation mechanism of Fe-doped TiO_2 microbelts

As shown in Fig. 2A, Fe-doped TiO_2 microbelts were synthesized. A mechanism of the formation of the Fe-doped TiO_2 microbelts is proposed. The formation mechanism of the Fe-doped TiO_2 microbelts is shown in Fig. 3.

There are abundant hydroxyl groups on the surface of cellulose of the absorbent cotton template. When the absorbent cotton is impregnated in the mixture of $Ti(OBu)_4$ and anhydrous ethanol, the hydrolysis reaction does not exist in the system for lack of enough water. Thus there are enough time to form hydrogen bonds between the –O– bond of $Ti(OBu)_4$ and the hydroxyl groups on the surface of cellulose of the absorbent cotton. As evaporating of the solvent, the concentration of $Ti(OBu)_4$ increases and forms thin layer on the surface of the absorbent cotton fibers. In this process, the hydrolysis reaction appears for bonding of $Ti(OBu)_4$ and acetylacetone in the mixture. And $Ti(OH)_4$ molecules join each other by hydrogen bonds. And the complex reaction appears for acetylacetone and Fe^{3+}. At the gel point, the cross-linking net-like dry TiO_2 gel forms with some solvent and product of hydrolysis enwrapped in it. In the dry process, both Fe-doped TiO_2 gel and the cotton fiber shrink with decreasing of the solvent. However, the shrinkage ratio of the Fe-doped TiO_2 gel and the cotton fiber was different. Thus the crack phenomenon appears on the surface of the dry gel. The crack swells with decreasing of the solvent. In the calcinations process, there exists large impulse force on the Fe-doped TiO_2 gel layer for the combustion of cotton fiber. Thus the Fe-doped TiO_2 layer breaks along the crack, and the Fe-doped TiO_2 belts are obtained.

3.2.2. Formation mechanism of polypyrrole/Fe-TiO_2 composite

Fig. 2B, C, D show the morphology of polypyrrole/Fe-doped TiO_2 composites. It is shown that the morphology of the obtained polypyrrole/Fe-doped TiO_2 composites is microbelt structure.

Under magnetic stirring, the pyrrole aggregates is broken down. As the result of the effect of sodium lauryl benzene sulfate, the most pyrrole molecules adsorb on the surfactant aggregates on the Fe-doped TiO_2 microbelts surface. The hydrophilic groups of the sodium lauryl benzene sulfate are adsorbed on the surface of the Fe-doped TiO_2 microbelts, and the pyrrole monomers are adsorbed on the lipophilic group. When the pyrrole monomer concentration is at a low scale, most pyrrole monomers polymerized on the surfactant aggregates of the Fe-doped TiO_2 microbelt surface. After the polymerization process, Fe-doped TiO_2 microbelts are enwrapped by the polypyrrole layer. With increasing of the pyrrole monomer concentration in the system, the excessive pyrrole polymerized in the free space between the Fe-doped TiO_2 microbelts. And some polypyrrole spherical particles appear in the system (shown in Fig. 4D). The detailed mechanism of the polypyrrole/Fe-doped TiO_2 composite formation was still not clear, and should be extensively studied in the future.

3.3. Photocatalysis properties of the samples

The absorbency curves of methyl orange degradation by samples are shown in Fig. 4. It could be seen that the photocatalytic efficiency of polypyrrole/Fe-doped TiO_2 are higher than that of neat Fe-doped TiO_2. With increasing of the molar ratio of polypyrrole/Fe-doped TiO_2 from 2:1 to 6:1, the photocatalytic activity decreases. However, the photocatalytic efficiency of the pure polypyrrole is lower than the other samples. The results suggest that the ratio of 2:1 is the optimum molar ratio.

As we all known, TiO_2 consists of valence band (VB) and conduction band (CB), and energy difference between these two levels is said to be the band gap (Eg). When semiconductors are excited by photons with energy equal to or higher than their band gap energy

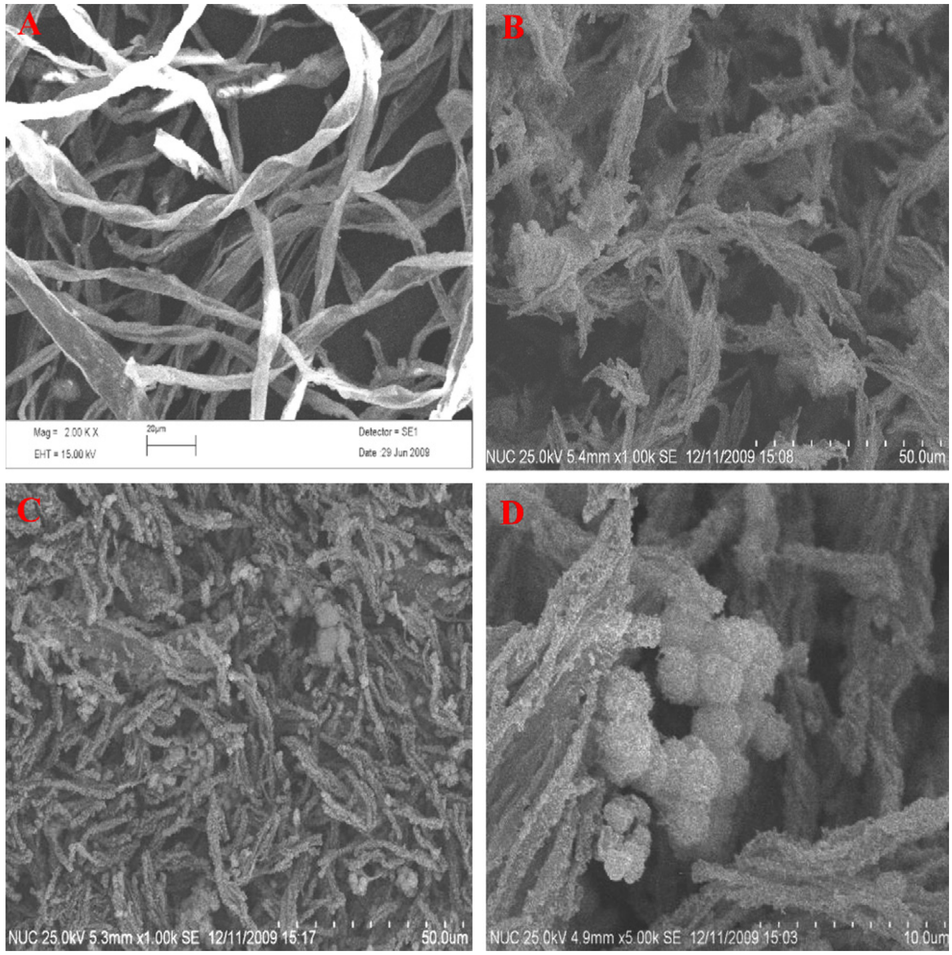

Fig. 2. The SEM images of the polypyrrole/Fe-doped TiO_2 composite obtained by different molar ratios of pyrrole/Fe-doped TiO_2: (A) 0; (B) 2; (C) 4; (D) 6; (E) ∞.

level, electrons receive energy from photons and thus are promoted from VB to CB if the gained energy is higher than the band gap energy level [21]. But the band gap of TiO_2 is so wide that it can be excited under UV light which is only 4–6% of sunlight.

It was reported that the band gap of Conducting polymers/TiO_2 nanocomposites is smaller than that of neat TiO_2 nanoparticles [22]. The narrow band gap allows polypyrrole/Fe-doped TiO_2 to adsorb more photons, and this will enhance the photocatalytic efficiency of Fe-doped TiO_2 under sunlight. When polypyrrole/Fe-doped TiO_2 composites are illuminated under sunlight, the electrons of polypyrrole/Fe-doped TiO_2 can be excited from the highest occupied molecular orbital (HOMO) to the lowest unoccupied molecular orbital (LUMO) of polypyrrole, and then the excited electrons can be injected to the CB of Fe-doped TiO_2, while holes will be left in

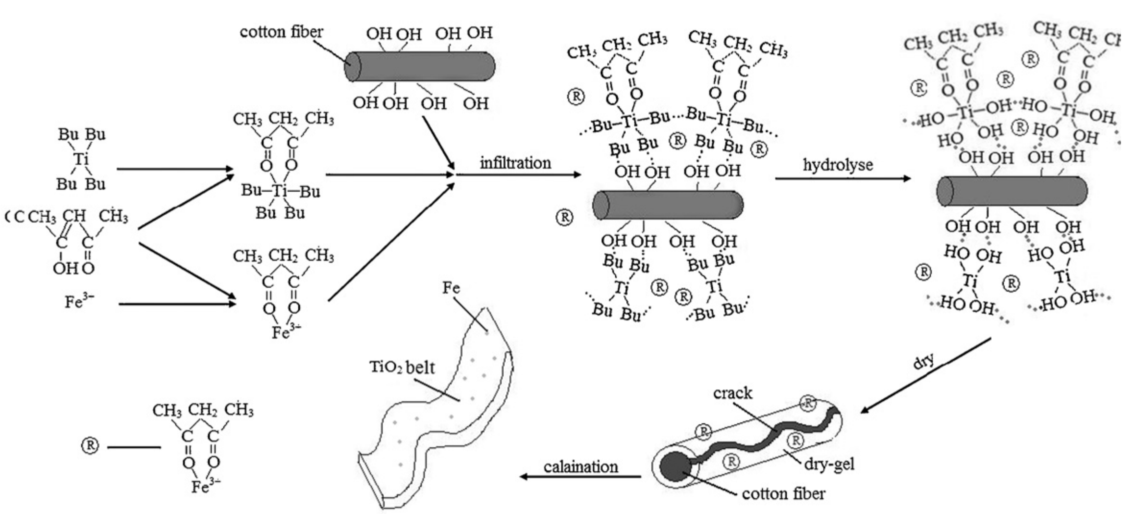

Fig. 3. The formation mechanism of the Fe-doped TiO_2 microbelt.

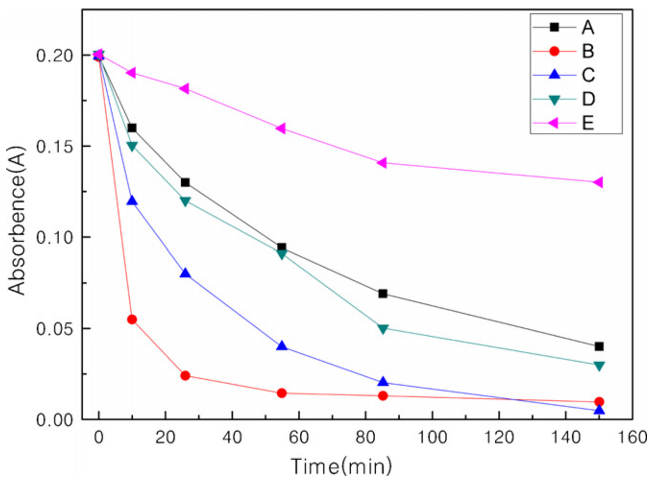

Fig. 4. The methylene orange degradation absorbency curves of the polypyrrole/Fe-doped TiO_2 composite obtained by different molar ratios of pyrrole/Fe-doped TiO_2: (A) 0; (B) 2; (C) 4; (D) 6; (E) ∞.

HOMO of polypyrrole. The electrons in VB of Fe-doped TiO_2 can migrate to the HOMO of polypyrrole to recombine with holes, and at the same time, holes generate in the VB of Fe-TiO_2. Thus, more and more photo-generated electrons and holes form in Fe-doped TiO_2 nanoparticles. The photogenerated electrons are so active that they can react with O_2 to generate ${O_2}^-$, and holes react with OH^- or H_2O to generate OH, these radicals can react with methyl orange. So polypyrrole plays a role as photosensitizer. The whole process can be clearly described in Fig. 5. The reactions can be expressed as follows:

$$\text{Polypyrrole-Fe-TiO}_2 \rightarrow \text{Polypyrrole}^+\text{-Fe-TiO}_2 + e^- \quad \text{(I)}$$

$$e^- + O_2 \rightarrow {}^\bullet {O_2}^- \quad \text{(II)}$$

$$\text{Polypyrrole}^+\text{-Fe-TiO}_2 \rightarrow \text{Polypyrrole-Fe-TiO}_2 + h^+ \quad \text{(III)}$$

$$OH^- + h^+ \rightarrow {}^\bullet OH \quad \text{(IV)}$$

$$H_2O + h^+ \rightarrow {}^\bullet OH + H^+ \quad \text{(V)}$$

However, with increasing of the molar ratio of polypyrrole/Fe-doped TiO_2 from 2:1 to 6:1, the photocatalytic activity decreases. It is because the Fe-doped TiO_2 microbelt is excessively enwrapped by the polypyrrole layer, which hinders the ultraviolet absorption characteristics of the composites [23]. Meanwhile, the thicker polypyrrole layers hinder the contacting between the hole and OH^-, H_2O, respectively, and further hider the formation process of $^\bullet OH$. Thus the photocatalytic activity decreases with increasing of the molar ratios of polypyrrole/Fe-doped TiO_2 from 2:1 to 6:1. So the sample with the ratio of 2:1 shows good photocatalytic efficiency.

3.4. The microwave absorptive properties

Fig. 6 shows the calculated reflection loss as a function of frequency for samples. The microwave absorbance of the samples

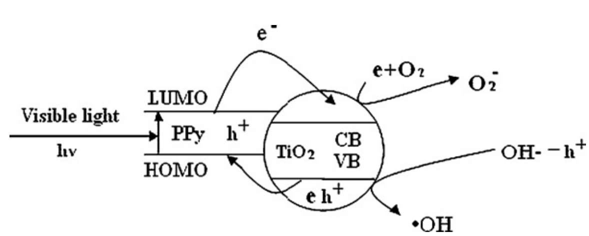

Fig. 5. The photocatalytic activity mechanism of polypyrrole/Fe-doped TiO_2 composite.

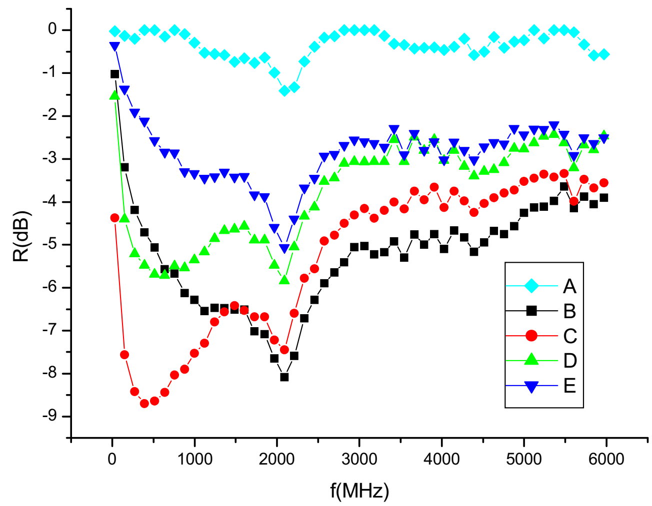

Fig. 6. Microwave loss spectra of the composites obtained by different molar ratios of pyrrole/Fe-doped TiO_2: (A) 0; (B) 2; (C) 4; (D) 6; (E) ∞.

could be predicted from R_L in which the larger the negative value of R_L, the greater the microwave absorption properties of materials [24]. The most important and interesting observation is that the reflection loss is found to depend sensitively on the molar ratio of the polypyrrole/Fe-doped TiO_2 composite. The reflection loss of the polypyrrole/Fe-doped TiO_2 composite increases firstly and then decreases with increasing of the polypyrrole content in the composite. The polypyrrole/Fe-doped TiO_2 composite posses excellent microwave absorption properties in the frequency band ranging from 30 to 3000 MHz. And the reflection loss of the sample C comes to −8.8 dB (410 MHz). The variation of the microwave absorption properties with the molar ratio of the polypyrrole/Fe-doped TiO_2 is ascribed to the variation of complex permittivity (ε'', ε'), complex permeability (μ'', μ') and loss tangent of dielectric/magnetic of the composite. The loss tangent ($\tan\delta$) of samples could be calculated from the real and imaginary parts of complex dielectric permittivity by using the formula $\tan\delta = \varepsilon''/\varepsilon'$. Materials with higher $\tan\delta$ are considered as lossy materials that indicate strong absorption. Thus, the value of loss tangent could predict the microwave absorbance of the material [25]. When the molar ratios of polypyrrole/Fe-doped TiO_2 range from 0 to 4:1, the increasing in the negative R_L attributed

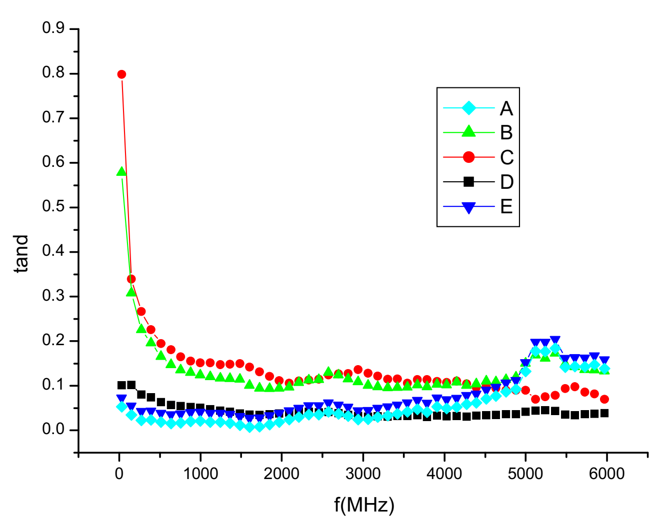

Fig. 7. Frequency dependences of the dielectric loss tangent ($\tan\delta$) of the composites obtained by different molar ratios of pyrrole/Fe-doped TiO_2: (A) 0; (B) 2; (C) 4; (D) 6; (E) ∞.

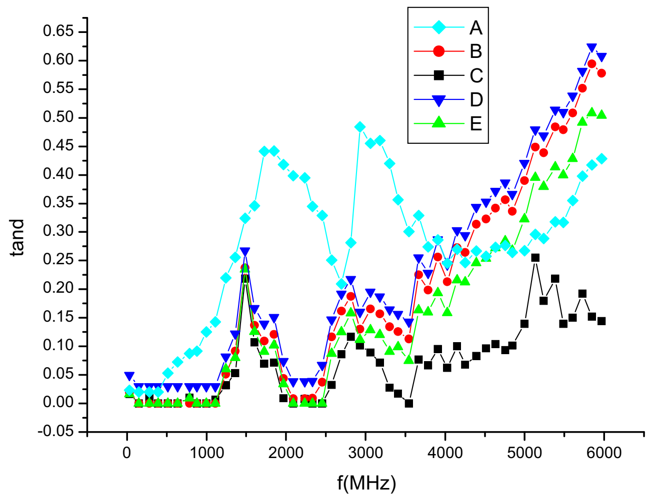

Fig. 8. Frequency dependences of the magnetic loss tangent (tan δ) of the composites obtained by different molar ratios of pyrrole/Fe-doped TiO_2: (A) 0; (B) 2; (C) 4; (D) 6; (E) ∞.

to the increasing of the value of loss tangent of dielectric of the composites. Fe-doped TiO_2 has higher ε' and equivalent ε. So the decreasing of Fe-doped TiO_2 will result in the slight decrease of ε' but cannot influence $\varepsilon''$of the composites (shown in Fig. 7). Thus the value of loss tangent of dielectric of the composites increases as the molar ratios of polypyrrole/Fe-doped TiO_2 ranging from 0 to 4:1. However, as the molar ratio of polypyrrole/Fe-doped TiO_2 is higher than 4:1, the negative R_L of the composite decreases with increasing of the molar ratio of polypyrrole/Fe-doped TiO_2. This is because of the decrease of μ'' resulting in decreasing of loss tangent of magnetic (shown in Fig. 8).

4. Conclusions

Polypyrrole/Fe-doped TiO_2 composites were prepared by in situ polymerization method. The possible formation mechanisms of Fe-doped TiO_2 microbelts and polypyrrole/Fe-doped TiO_2 composites had been proposed. The effect of the molar ratio of pyrrole/Fe-doped TiO_2 on the microwave loss properties and photocatalysis properties of the composites was studied. It indicates that the optimum molar ratio of pyrrole/Fe-doped TiO_2 was 2:1 to obtain the sample with both excellent microwave loss properties and good photocatalysis properties.

Acknowledgements

This work was supported by the National Nature Science Fund (20571066, 20871108), program for the Top Science and Technology Innovation Team of Higher Learning Institutions of Shanxi, and program for the Top Young Academic Leaders of Higher Learning Institutions of Shanxi.

References

[1] P.M. Dziewonski, M. Grzeszczuk, Electrochim. Acta 55 (2010) 3336–3347.
[2] J. Wang, X. Ni, Solid State Commun. 146 (2008) 239–244.
[3] P. Wang, T. Xie, L. Peng, H. Li, T. Wu, S. Pang, D. Wang, J. Phys. Chem. C 112 (2008) 6648–6652.
[4] C. Wei, Y. Zhu, X. Yang, C. Li, Mater. Sci. Eng. B 137 (2007) 213–216.
[5] X. Ma, M. Wang, G. Li, H. Chen, R. Bai, Mater. Chem. Phys. 98 (2006) 241–247.
[6] Z. Liu, W. Guo, D. Fu, W. Chen, Synth. Met. 156 (2006) 414–416.
[7] G.K.R. Senadeera, T. Kitamura, Y. Wada, S. Yanagida, J. Photochem. Photobiol. A 164 (2004) 61–66.
[8] S. Ameen, M.S. Akhtar, G.-S. Kim, Y.S. Kim, O.B. Yang, H.-S. Shin, J. Alloys Compd. 487 (2009) 382–386.
[9] L. Hong, Y. Li, M. Yang, Sens. Actuators A 145 (2010) 25–31.
[10] U. Lange, N. Roznyatovskaya, V. Mirsky, Anal. Chim. Acta 614 (2008) 1–26.
[11] A. Fujishima, X. Zhang, D.A. Tryk, Surf. Sci. Rep. 63 (2008) 515–582.
[12] Y. Lv, L. Yu, H. Huang, H. Liu, Y. Feng, J. Alloys Compd. 488 (2009) 314–319.
[13] Y.F. Tu, S.Y. Huang, J.P. Sang, X.W. Zou, J. Alloys Compd. 482 (2009) 382–387.
[14] M.C. Wang, H.J. Lin, T.S. Yang, J. Alloys Compd. 473 (2009) 394–400.
[15] R. Caruso, M. Giersig, F. Willig, M. Antonietti, Langmuir 14 (1998) 6333–6336.
[16] X. Li, T. Fan, H. Zhou, S. Chow, W. Zhang, D. Zhang, Q. Guo, H. Ogawa, Adv. Funct. Mater. 19 (2009) 45–56.
[17] F. Wang, S. Min, Y. Han, L. Feng, Superlattices Microstruct. 48 (2010) 170–180.
[18] Y. Tong, Y. Li, F. Xie, M. Ding, Polym. Int. 49 (2000) 1543–1547.
[19] K.S. Jang, H. Lee, B. Moon, Synth. Met. 143 (2004) 289–294.
[20] B. Birsöz, A. Baykal, H. Sözeri, M.S. Toprak, J. Alloys Compd. 493 (2010) 481–485.
[21] X. Chen, S.S. Mao, Chem. Rev. 107 (2007) 2891–2959.
[22] M. Ni, M.K.H. Leung, D.Y.C. Leung, K. Sumathy, Renew. Sust. Energy Rev. 11 (2007) 401–425.
[23] D. Wang, Y. Wang, X. Li, Q. Luo, J. An, J. Yue, Catal. Commun. 9 (2008) 1162–1166.
[24] D. Makeiff, T. Huber, Synth. Met. 156 (2006) 497–505.
[25] S. Phang, R. Daik, M. Abdullah, Thin Solid Films 477 (2005) 125–130.